International Journal on Advanced Science Engineering Information Technology

Vol.13 (2023) No. 4
ISSN: 2088-5334

Experimental Study of Different Materials on Electromagnetic Damping Characteristics

M.F. Mohd Yusoff [a,*], A.M. Ahmad Zaidi [b], S.A. Firdaus Ishak [a], M.K. Awang [a], MF Md Din [a], A. Mukhtaruddin [a], A.M. Ishak [a]

[a] *Faculty of Engineering, National Defence University of Malaysia, Sg. Besi Camp, Kuala Lumpur, Malaysia*
[b] *Faculty of Defence Science and Technology, National Defence University of Malaysia, Sg. Besi Camp, Kuala Lumpur, Malaysia*
*Corresponding author: *fazli@upnm.edu.my*

***Abstract*—Electromagnetic damper has been given special attention by many researchers and thus is among the important research areas in vibration system. This paper examines electromagnetic damper effect through simulation and experimental study. A vibration test rig incorporating a simple electromagnetic damper is designed and tested to examine the impact of electromagnetic force.The vibration system test rig can be operated as free vibration as well as a forced vibration system. In the simulation phase, the MATLAB model of the electromagnetic damper system is developed, considering its dynamic behavior. This simulation allows for the evaluation of the damper's effectiveness in reducing vibration amplitudes and settling times. Subsequently, an experimental setup is constructed to validate the simulation results. One of the key findings of this research is the comparison of different materials used as the outer cylinder of the electromagnetic damper system. The results indicate that aluminum exhibits a superior damping coefficient value of 2.8 kgs^{-1} compared to Nylon, which has a damping coefficient of 1.9 kgs^{-1}. This observation highlights the significant impact of the damper's material choice on the vibration system's amplitude and settling time. The implementation of aluminum as the outer cylinder results in reduced amplitudes and quicker settling times in the vibration system. The combination of simulation and experimental studies enhances the understanding of the electromagnetic force's influence and validates the findings. The comparison of different materials for the damper's outer cylinder underscores the importance of material selection in achieving optimal damping coefficients and improved vibration system performance.**

***Keywords*— Electromagnetic damper; eddy current; vibration; suspension system; MATLAB.**

Manuscript received 3 Sep. 2022; revised 6 Oct. 2022; accepted 7 Nov. 2022. Date of publication 31 Aug. 2023.

I. INTRODUCTION

Problems and issues in vibration, such as fatigue, fracture, and energy loss, are the subject matters to be addressed by an engineer in this area. Engineers are combatting those issues by keeping on improving the vibration-damping response by adjusting the isolation system. The undesirable vibration will cause damage or fracture to a system. For example, the excessive vibration presented in the car will induce harmful wear on the car's components [1]. Traditionally, in a vehicle's suspension system, damper and spring is the main element being investigated to obtain the best performance of a car in terms of ride and handling as well as to withstand the car's weight.

Vibration and suspension are two elements that are very common in suspension systems. Suspension can be categorized into passive, semi-active, and active systems. Each type of system has its own pros and contra. However, most researchers are looking into a semi-active system since the passive system can be tuned only during manufacturing while the active system is complex and costly.

Suspension systems can be classified as passive, active, or semi-active based on the level of controllability[2]. All of them utilize the spring and damper units. Most of the suspension systems proposed and implemented in vehicle suspension systems are based on hydraulic or pneumatic devices [3]. Classification of suspension systems is based on their capability to take in, contribute to, or remove energy. The conventional passive suspension has an absorber as a damper and a spring to communicate with sprung mass and unsprung mass [2], [4]. The response of this system depends on the damping and spring constant value that has been fixed during the setup [5].

A suspension system consists of a spring, damper, and structural components carrying (links) the sprung mass (car chassis). The spring stores energy, the shock absorber dissipates energy proportional to its damping coefficient, and the links restrict the suspension system and limit motion[6]. A suspension system is used as part of a vehicle system because it has several tasks to perform during the vehicle's movement. Generally, conflicting demand requirements for a suspension system are to provide a comfortable ride, isolate the vehicle body from road irregularities, enhance the ride handling by producing a continuous road-wheel contact, and support the vehicle weight [6]. Good handling requires a suspension setting that is neither stiff nor soft. A soft suspension is required for a comfortable ride, but it must be responsive to changes in applied loads. The classic passive suspension consists of a constant coefficient spring and damper. Due to these opposing requirements, the suspension design should achieve a balance between the two, as seen in Fig. 1.

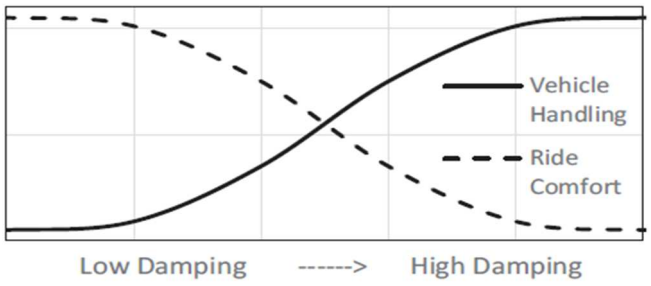

Fig. 1 Vehicle handling and ride comfort in passive suspension[7]

Most of the suspension systems that are proposed and implemented in vehicle suspension systems are based on hydraulic or pneumatic devices [3], [8] which have several drawbacks such as hose leaks and ruptures. It is also inefficient due to the required continuously pressurized system [9].

Thus an alternative way to avoid all the issues pertinent to hydraulic usage is to study the electromagnetic damping which is an oil-free, no mechanical contact, high reliability, and stability that is applicable in various vibration isolation systems such as precision machinery, micro-mechanical suspension systems, and structure vibration isolation [10]–[12].

In Abdo et al. [12], a model is developed for a proposed eddy current damper using finite element analysis. In this research, the proposed eddy current damper being added to the traditional damper and the effectiveness of the damper being investigated through the quarter car MATLAB simulation by comparing the with and without eddy current damper result.

The effect of electromagnetic can be divided into two phases. The first one is due to the eddy current induced in the system by considering Faraday's Law theory. The other effect that can be tested under this concept is by creating a solenoid such that it will interact with the permanent magnet.

An eddy current is caused when a moving conductor intersects a stationary magnetic field or vice versa. The relative motion between the conductor and magnetic field generates the eddy current circulation within the conductor. The flow of electrons in the conductor immediately creates an opposing magnetic field, generating Lorentz forces, which dampen the magnet motion and produce heat inside the conductor [13], [14]. These circulating eddy currents induce their magnetic field, causing a resistive force [15]. Even though eddy current can be used as a damper, some issues still need to be addressed, such as magnetic contamination and heat generation [14]. It also increased the volume of the suspension since the force density of the active part of hydraulics is higher than for electromagnetic actuation, and also higher system cost due to the expensive cost of the permanent magnet [16]. Thus, this phenomenon needs to be investigated to determine whether it can benefit or harm any dedicated system. In this research, the effect of different material to be used as electromagnetic dampers would be investigated experimentally using a one-degree-of-freedom vibration test rig.

A. General Concept of Electromagnetic Damper

Various research and development were related to electromagnetic damping [1], [3], [11], [17], [18]. Eddy currents are one case of electromagnetic induction. Eddy current damper has the advantage of contactless damping that does not require physical contact to produce a damping force that can prolong the damper's life. It will not have a problem with fluid leakage nor be affected by the rise in temperature. The magnetic flux between the magnet and the conductor inside an eddy current damper can be used to generate power[19].

Sodano et al. [20] studied the application of an eddy current damper (ECD) in controlling the vibrations of a small cantilever beam. While some other studies [12], [14], [16], [21]–[30] revealed the application of eddy current dampers as vibration control systems in vehicles and structures. Gysen et al. [16] studied the availability of linear motors in active EMS. In their paper, a tubular permanent magnet actuator (TPMA) has been deployed in an experimental one-degree of freedom (1 DOF) quarter-car setup, as shown in Fig. 2.

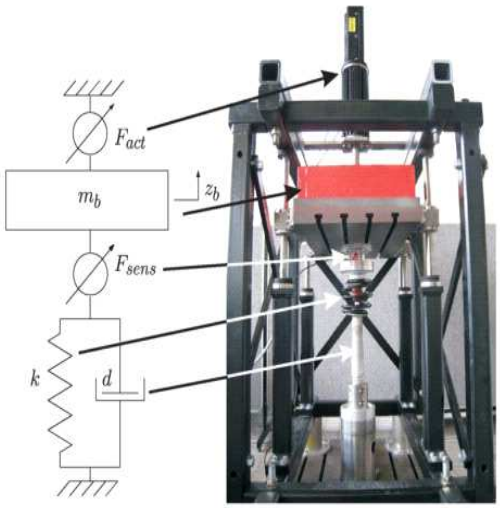

Fig. 2 Quarter car test setup and its schematic diagram[16]

The thrust force can be generated actively by supplying the external voltage inside the armature winding. The active armature then interacts with a permanent magnet translator, thus causing linear movement. Asadi et al.[31] has developed

a prototype of an adaptive and regenerative damper which was categorized as a hybrid electromagnetic damper is proposed. The hybrid damper is configured to operate with viscous and electromagnetic subsystems. The electromagnetic component was modeled and analyzed using analytical (lumped equivalent magnetic circuit) and Finite element method (FEM) software, namely COMSOL, and investigated experimentally. The simulation and experiment results show that the damper can produce damping viscous coefficients of 1300 Nsm^{-1} and 0–238Nsm^{-1} for the electromagnetic damping.

A mechanism such as a ball screw and nut are needed to convert the linear movement into rotational movement. Montazeri et al. [32] investigate the feasibility of an electromagnetic damper (EMD) in providing adequate damping for vibration isolation while generating energy from relative motion between sprung and unsprung masses. The electromagnetic damper (EMD), which is composed of a permanent-magnet DC motor, a ball screw, and a nut, is considered to be analyzed as a passive damper in a quarter-car model. It has been shown through simulation that the designed passive EMD maintains the desired performance while external excitation from road excitation can be regenerated and transformed into electric energy.

A one-degree of freedom (1 DOF) vibration isolation system test rig has been developed to test an eddy current damper [33]. The eddy current damper is being developed by considering the permanent magnet design configuration. An analytical model of the induced eddy current force is derived by applying electromagnetic equations. The prototype of the system has been developed and tested, showing an improvement tenfold in the damping characteristics of a 1DOF isolation system.

In Fow and Duke [34], a passive linear electromagnetic damper created using a permanent magnet and coil system is developed and validated on a small scale. It is then being tested in a one-degree-of-freedom system test rig as shown in Fig. 3 below.

Figure 5. A small scale test rig with signal analyser. (1) is the spring, (2) the coil, (3) is a mass attached to the magnet, which is inside the coil. These are then connected to the spring. The accelerometer (4) is connected to the signal analyser (5).

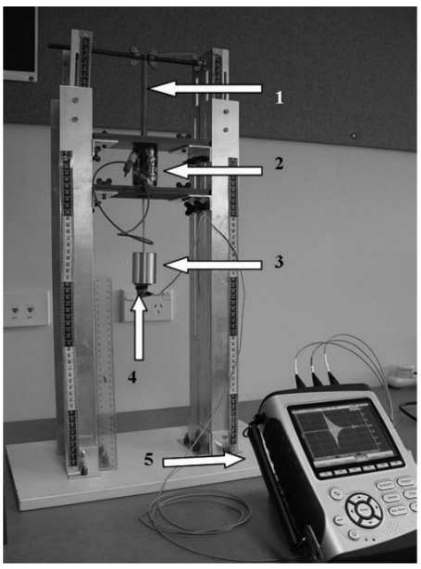

Fig. 3 A small test rig was constructed for initial validation of the damper model [34]

The magnet was modeled numerically as an air-cored solenoid, and the flux generated by the magnet is determined over the range of displacement for the masses. It was recorded as a lookup table for use in the dynamic model. The dynamic model was further scaled up as a two-degree of freedom system to determine the damping for a quarter car model. The proposed damper could produce a damping coefficient of 1,600 Ns/m but unfortunately, it required more than three times the volume of the equivalent hydraulic dampers[34]

In Hyniova [27], an electromagnetic linear motor was used as an actuator in active suspension systems. A control algorithm using H∞ controller was used in conjunction with the designed linear motor model such that the required electric power necessary to be supplied or consumed when the velocity and force of the motor are constant.

An analytical model of nonlaminated axisymmetric cylindrical electromagnetic suspension system has been developed by considering six elements in the rotor, coil and flotor design [35]. The model obtained is a fractional-order system as a fractional-order power of variable s appears in the denominator of the output (position of the flotor) over input (perturbation current) of the transfer function.

A rack– pinion-based electromagnetic damper regenerative was developed and tested experimentally[36]. The dynamic modelling of the system was done by considering an electric motor as a generator such that a steady power of voltage can be captured. The research was further prolonged by having a prototype in the experimental work. The experiment results indicate that the generated voltage has a peak power of 67.5 W and an average power of 19.2W. This experiment was done when the vehicle traveled 48 km/h (30 mi/h) on a smooth campus road.

The basic idea of this research is to create a magnetic flux interaction between the permanent magnet and hollow cylinder, which surrounds the permanent magnet movement. The permanent magnet moves vertically through the electromagnetic damper (a coil wound in a hollow cylinder), as being shown in Fig. 4.

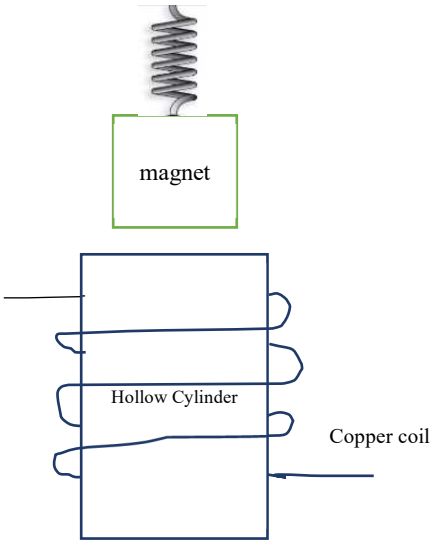

Fig. 4 Schematic diagram of the main effect occurs.

Ring-shaped ferrite magnets attached to an aluminum rod act and a spring acted as a translator moving through the hollow cylinder, which wounded with copper coil. Thus, an

electromagnetic induction will be inducted into the wounded cylinder due to a changing magnetic field. An Eddy current will be induced according to Faraday's law conductor in response to a changing magnetic field [34], [37], [38].

According to Michael Faraday's experiment, a static magnetic field does not create current flow. However, a time-varying magnetic field in a closed loop produces an induced voltage or electromotive force. Faraday's law can be summarized as the induced electromotive force, V_emf (in unit Volts), in a closed circuit is equal to the rate of change of magnetic flux linkage by the circuit[39]. The equation can be expressed as follows.

$$V_{emf} = -N\frac{d\emptyset}{dt} \quad (1)$$

where N is the number of turns in the circuit, which consider an N-turn filamentary conductor of the closed path and ϕ is the magnetic flux (in unit Weber) through each turn. The negative sign is based on Lenz's law which states that an induced electromotive force produces current opposed to the direction of the change of magnetic flux that induced it. Fig. 1 shows that the magnets are moving up and down in the coil. According to Faraday's law, the change of magnetic flux will induce an electromagnetic force in a closed circuit. Therefore, the changing magnetic flux due to the moving magnets repeatedly will produce an alternating voltage in the coils.

From that, magnetic flux, ϕ is defined as the amount of magnetic field lines passing through a given closed surface.

$$\Phi = \int_s B.dS \quad (2)$$

where B is the magnetic magnetic flux density in unit of Tesla and dS is the element of the surface [39].Based on the Maxwell-Faraday equation, the electromagnetic induction can be explained. The Maxwell-Faraday equation states the following equation.

$$\nabla \times \vec{E} = -\frac{\partial B}{\partial t} \quad (3)$$

This means the electric field curl is equal to the partial derivative of the magnetic field. If this equation is integrated over a plane surface:

$$V_{emf} = \oint E.dL = \frac{d}{dt}\int_s B.dS \quad (4)$$

The resulting electric field in the contour of the area is equal to the changing of magnetic flux responding to time and both sides are equal to a voltage. This show that the electric current or voltage can be produced when a changing magnetic field within a stationary loop or a constant magnetic field with a moving loop[39].

The force between magnet and electromagnet can be considered as follows:

$$F = \int_\Gamma J\ x\ B\ d\Gamma \quad (5)$$

where Γ, J and B are the conductor's volume, induced current density and magnetic flux density, respectively. The induced current density J in the conductor is calculated as follows, assuming a constant magnetic flux density:

$$J = \sigma(VXB) \quad (6)$$

where σ and v are the conductor's conductivity and the relative velocity of the magnetic flux density and the conductor, respectively.

As shown in Equation (6), the induced current density (J) depends on three factors, first conductivity of medium (σ), second the relative vertical velocity between the stator and the conductor (v), and the flux density (B). Thus, according to the Lorentz force law, the relative movement of the magnets and the conductor causes the eddy currents to induce in the conductor, producing the magnetic flux that opposes the external magnetic flux density, resulting in a damping force per each pole piece [40].

B. Damping Ratio ξ Calculation Through Vibration Response

The damping ratio ζ is a dimensionless measure describing how oscillations in a system decay after a disturbance. The damping ratio is a measure describing how rapidly the oscillations decay from one bounce to the next. The damping ratio is a system parameter, denoted by ζ (zeta), that can vary from undamped (ζ = 0), underdamped (ζ < 1) through critically damped (ζ = 1) to overdamped (ζ > 1). In this experiment, damping ratio will be determined through logarithmic decrement due to the system being underdamped. The period of oscillation, T, is the time between two peaks. Can be calculated as [11].

$$T = \frac{t_n - t_0}{n} \quad (7)$$

where t_n is the time at which the nth peak occurs, as shown in Fig. 5, the nth peak occurs at time t_n.

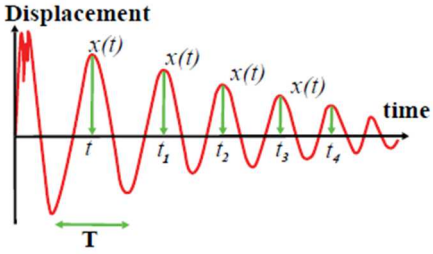

Fig. 5 Displacement versus time in free vibration damped oscillations [11]

The logarithmic decrement can be defined as follows[14].

$$\delta = \log\left(\frac{x(t_n)}{x(t_{n+1})}\right) \quad (8)$$

where $x(t_n)$ is a displacement located at the n^{th} peak. From T and δ in equation 7 and 8, the damping ratio, ζ can be calculated as follows.

$$\zeta = \frac{\delta}{\sqrt{4\pi^2 + \delta^2}} \quad (9)$$

C. Damping Coefficient, C

The system's damping coefficient measures how quickly it returns to rest as the frictional force dissipates its oscillation energy. The damping coefficient can be determined by applying the values of damping ratio, mass of sprung mass

and spring stiffness. From damping ratio, ζ in equation 9, The value of damping constant will be affected the value of damping ratio ζ according to the equation below.

$$\zeta = \frac{\delta}{\sqrt{(4\pi)^2+\delta^2}} = \frac{c}{2\sqrt{mk}} \tag{10}$$

where, m=mass, k= spring stiffness and *c*= damping coefficient.

II. Materials and Method

A. Materials

This paper uses an experimental approach to show the effect of different material in the electromagnetic damper. First, a vibration test rig has been designed to be regarded as a mass spring damper system. The experimental testing is being run with two different materials (Aluminum and Nylon) of electromagnetic damper. Two types of electromagnetic damper from Aluminum and Nylon have been fabricated and tested using the test rig. Fig. 6 shows different types of material as electromagnetic damper with 900 turns of copper wire coil. The copper wire has an insulator around it such that it will not create short circuit in the connection. The dimensions of those two cylinders are the same, 220mm in length, 76mm outer diameter and 66mm inner diameter.

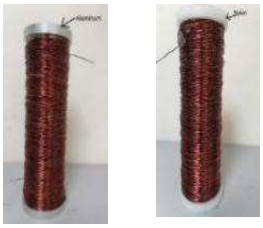

Fig. 6 Two different cylindrical materials (Aluminum and Nylon) for electromagnetic damper

The result was extracted and analyzed such that the effect of different material can be clearly shown from the experimental result. The system's parameter has been extracted using the logarithmic decrement method. After that, a simulation using MATLAB software was done to visualize the effect of damping coefficient more clearly.

B. Experimental Test Rig of Electromagnetic Damper

The overall test rig system components can be seen in Fig. 7. Basic components of the system are electromagnetic damper, sensor, spring, linear bearing, permanent magnet, LMS Data Acquisition System and LMS Test Express Software[41]. The spring and linear bearing make the system oscillate vertically once it has been excited. A permanent magnet has been attached at the end of the shaft. The dimensions of the ferrite magnet are 22mm (inner diameter), 45mm (outer diameter), and 8 mm (thickness of each magnet). The vibration response of the system was taken through the accelerometer sensor which connected to LMS DAQ and LMS Test Express Software[42]. The acquired response was acceleration response of a mass spring damper system which can be integrated to obtain velocity and displacement response of the system. The electromagnetic damper as a subject of investigation has been located at the bottom of the test rig to interact with the permanent magnet, which oscillated as the system being excited.

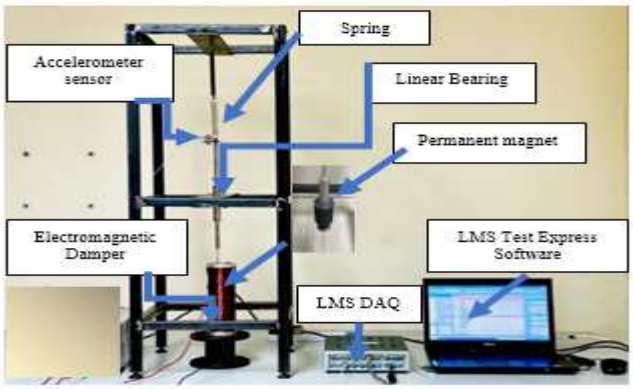

Fig. 7 Overall vibration test rig system

III. Results and Discussion

Several trial runs were done, and the best result was captured such that it could be analyzed. Figures 8 and 9 show the response obtained from the vibration test rig for a 6cm and 8cm initial displacement response. The initial displacement was arbitrarily chosen from the maximum displacement available based on the test rig capabilities. It was chosen such that the effect of vibration can be clearly obtained, and the effect of the electromagnetic damper can be illustrated through the experiment.

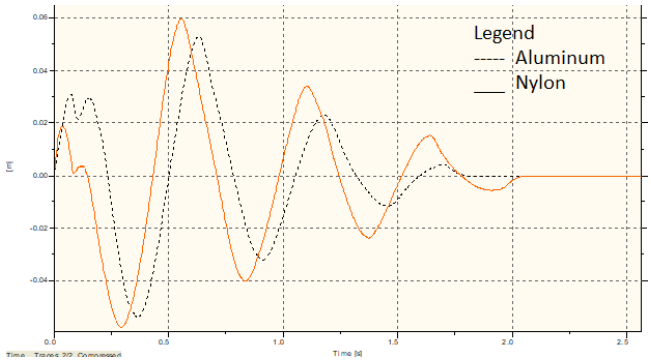

Fig. 8 Six (6) cm response for nylon (higher amplitude response) and aluminum (lower amplitude response

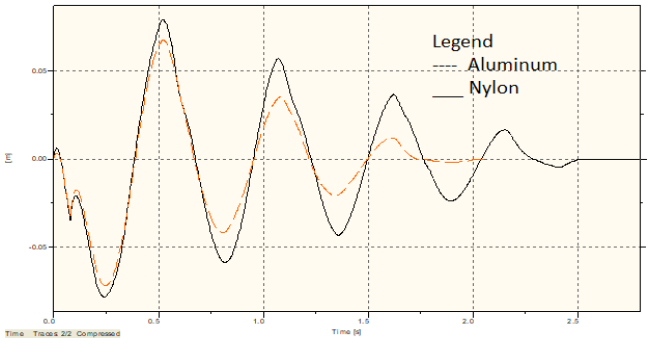

Fig. 9 Eight (8) cm response for nylon (higher amplitude response) and aluminum (lower amplitude response)

The data has been extracted and analyzed to identify the exact value of the peak using MS Excel. Fig. 10 to 13 show all the responses.

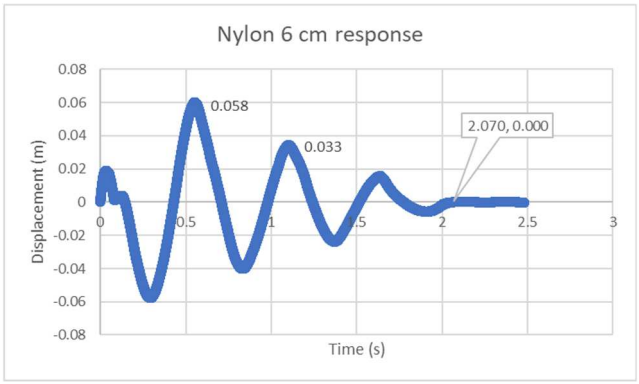

Fig. 10 Nylon 6cm response

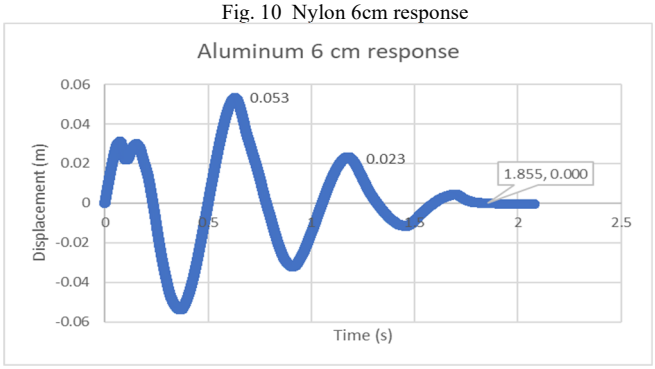

Fig. 11 Aluminum 6 cm response

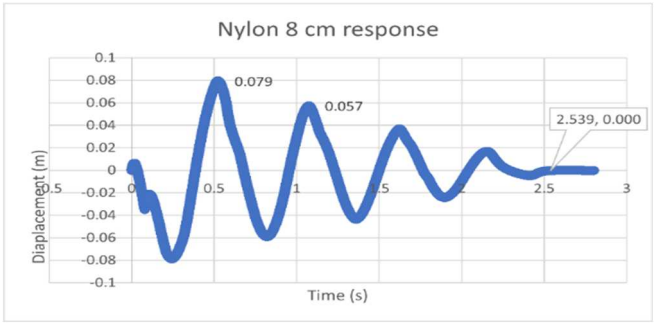

Fig. 12 Nylon 8 cm response

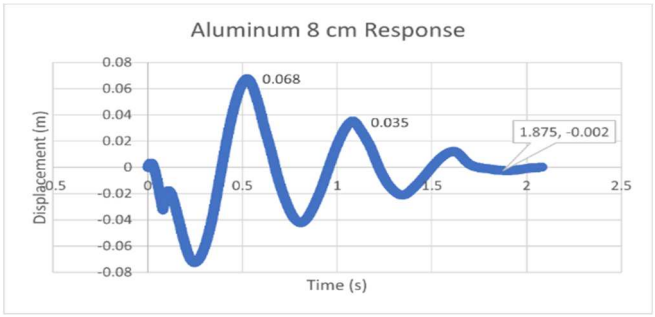

Fig. 13 Aluminum 8 cm Response

For comparison purposes all the responses have been tabulated in Table 1. Aluminum gives the highest value of damping ratio and coefficient. This can be interpreted by looking at the settling time, damping coefficient and amplitude of the vibration response.

TABLE I
VIBRATION RESPONSE DUE TO DIFFERENT MATERIALS AND AMPLITUDES (CM)

Material	Aluminum		Nylon	
Initial Amplitude (cm)	6 cm	8 cm	6 cm	8 cm
Logarithmic decrement, δ	0.87	0.67	0.59	0.33
Damping ratio, ζ	0.137	0.106	0.093	0.052
Damping coefficient, c (kgs^{-1})	2.8	2.17	1.9	1.05
Time taken to achieve steady state, t_s (s)	1.85	1.87	2.07	2.54

A. MATLAB Simulation of the Vibration Test Rig System

The vibration test rig system with the electromagnetic damper has been considered as a mass spring damper system as shown in Fig. 14.

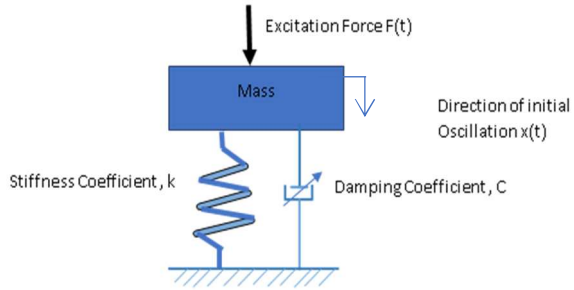

Fig. 14 Diagram of mass spring damper system being excited by a force.

The equation of motion derived based on Fig. 13 can be written as follows.

$$\ddot{x} = \frac{1}{m}(F - c\dot{x} - kx) \tag{11}$$

The second order ordinary differential equation can be represented in state space form of $\dot{X} = AX + Bu$ by considering the displacement x(t) and velocity $\dot{x(t)}$ as the state vector and F(t) as and input vector such that $X_1(t) = X(t)$, $X_2(t) = \dot{X}(t)$ and $u(t) = F(t)$.

Rearrange the equation into a matrix form such that:

$$\dot{X_1}(t) = X_2(t) \tag{12}$$

$$\dot{X_2}(t) = -\frac{k}{m}X_1(t) - \frac{c}{m}X_2(t) + \frac{1}{m}u(t) \tag{13}$$

This equation can be represented as a state space equation as below.

$$\begin{bmatrix} \dot{X_1} \\ \dot{X_2} \end{bmatrix} = \begin{bmatrix} 0 & 1 \\ -k/m & -c/m \end{bmatrix} \begin{bmatrix} X_1 \\ X_2 \end{bmatrix} + \begin{bmatrix} 0 \\ 1/m \end{bmatrix} [u(t)] \tag{14}$$

The effect of damping and spring constant has been plotted in MATLAB software as in Fig. 15. The value of damping constant will be affected by the damping ratio ζ value according to the equation 10 previously. As can be seen in Fig. 15, the damping ratio ζ which is directly related to the damping coefficient, c plays an important factor for the vibration response. For instance, the lower value of c (500 Ns/m) will produce an underdamped oscillation response. The amplitude of the vibration decays over time. In contrast, the bigger value of c (4500 Ns/m) will produce a response that will decay more quickly than the underdamped response. The larger damping leads to quicker energy dissipation and prevents the system from vibrating.

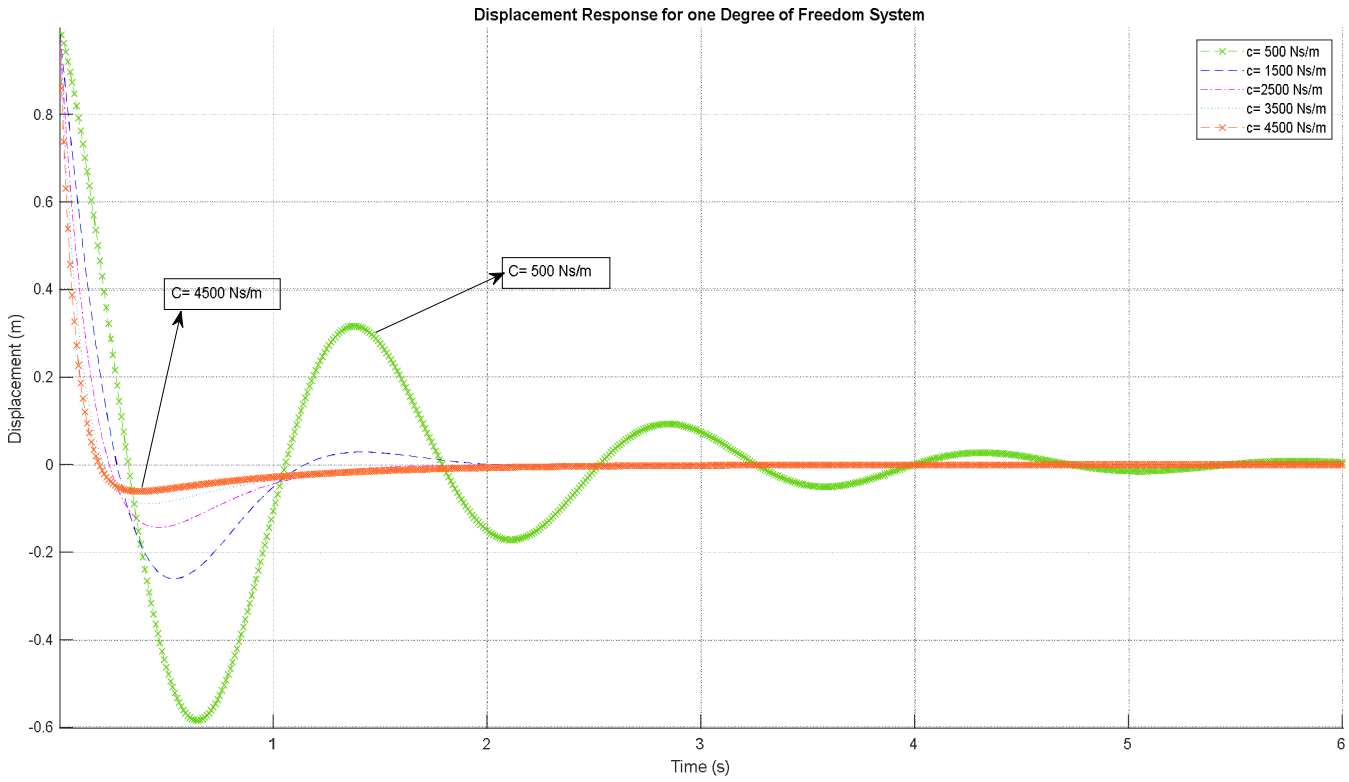

Fig. 15 Displacement response for one degree of freedom (DOF) system

B. Damping Coefficient, C of the System

The experimental results clearly show that the damping coefficient value affects the vibration response. It can be traced from the damping coefficient, C of the system, and the settling time of the response. Settling time for some aluminum from a 6 cm response was only 1.85 seconds. In contrast, for a Nylon electromagnetic damper, the time was slightly longer, around 2.07 to 2.54 seconds. This is in line with the simulation obtained for the one degree of freedom system using MATLAB which indicated that the vibration response is affected by the damping coefficient, c value.

Another point that can be pointed out is that the damping coefficient, c, exists in the actual electromagnetic damper system. This can be traced out by looking at the response obtained as in Fig. 8 and 9. Thus the assumption deployed for the MATLAB simulation as in Fig. 14 makes sense. The damping coefficient, C, has been varied such that the vibration response can be controlled. If this result is being used for a suspension system, the displacement amplitude of the sprung mass can be controlled. A lower amplitude will give less disturbance to the passenger of the car. The passenger will not feel the bouncing effect due to the road input. Thus, the car will become more stable during the movement of the car. Passengers will become more comfortable while cruising with the car.

From the experimental result, material of the electromagnetic damper should be considered to generate higher magnetic flux value. This effect can be related to the material's permeability, which allows the magnetic lines of force to pass through it. For instance, the permeability value for aluminum is 1.256 μH/m while for nylon is less than 1 [43]. Thus, creating a bigger value of magnetic flux density. The magnetic lines will produce the magnetic flux density, B as being indicated by the equation [39].

$$B = \mu_o nI \tag{15}$$

$$n = \frac{N}{L} \tag{16}$$

where $\mu_o = 4\pi \times 10^{-7}$ Tesla, T is the constant magnetic of permeability of magnet in free space I = the current in ampere, A, N = the number of turns of coil and L = the length of solenoid.

The novelty of this research was indicated by relating the vibration system response (mass, spring damper system) with the electromagnetic damping coefficient C, effect. The vibration response of the system (displacement response) is being analyzed through the logarithmic decrement method such that it can be related to the damping coefficient c, of the system.

From vibration system point of view, the damping coefficient, c of a mass spring damper system can be obtained from a general equation of, F=cv where $c = 2\pi a \frac{N^2 B_{rad}}{R}\left(\frac{d\emptyset}{dt}\right)\frac{1}{v}$. This is the general equation which related the force of the damping with the damping coefficient (c) and velocity (v). This expression is taken from the effect of permanent magnet moving vertically towards a coil of wire as discussed by Saslow's [30]. Fig. 16 shows the schematic diagram of the phenomenon. In this diagram, a permanent magnet moves vertically at a certain velocity towards a col of wire such that an induced current is induced into the coil.

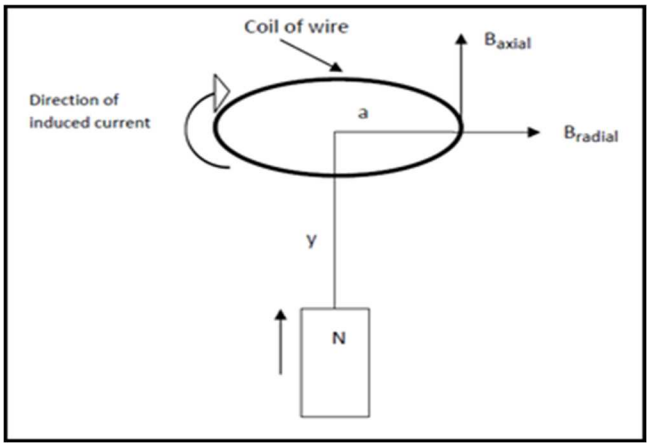

Fig. 16 Schematic diagram for magnetic force

Thus, the result obtained in Table I indicated that the magnetic flux density (B) in the system will affect the damping coefficient, C value. It has been shown that, by considering some aluminum as the cylindrical material in electromagnetic damper the damping coefficient c of the system can be increased.

IV. Conclusion

This paper has demonstrated the effect of different materials that can be used in electromagnetic damper fabrication; materials such as nylon and aluminum have been investigated in this research. It has been shown that aluminum can generate a bigger damping coefficient value than nylon. The damping coefficient of aluminum (2.8 kgs^{-1}) is better than Nylon (1.9 kgs^{-1}) because the permeability value of aluminum is greater than Nylon. Thus, the interaction between the permanent magnet and the aluminum cylinder created a bigger damping force. The output from the experimental part has been extracted and analyzed through the logarithmic decrement equation. The result from MATLAB simulation has been verified such that the effect of damping coefficient can be shown from a vibration system's mass spring damper response.

It can be concluded that this magnetic damper can absorb the vibration by using an electromagnetic force and a strong permanent magnet. The response time for the system to damp out will be affected by the type of material used in the system. This effect can be verified by calculating the damping value in the logarithm decrement equation.

Acknowledgment

The authors thank UPNM through Research Grant: FRGS/1/2020/STG07/UPNM/03/2 and short-term research grant: UPNM/2016//GPJP/5/TK/5.

References

[1] Q. Cai and S. Zhu, "Enhancing the performance of electromagnetic damper cum energy harvester using microcontroller: Concept and experiment validation," *Mech. Syst. Signal Process.*, vol. 134, p. 106339, Dec. 2019, doi: 10.1016/j.ymssp.2019.106339.

[2] M. A. A. Abdelkareem *et al.*, "Vibration energy harvesting in automotive suspension system: A detailed review," *Appl. Energy*, vol. 229, no. April, pp. 672–699, Nov. 2018, doi: 10.1016/j.apenergy.2018.08.030.

[3] S. Li, J. Xu, X. Pu, T. Tao, H. Gao, and X. Mei, "Energy-harvesting variable/constant damping suspension system with motor based electromagnetic damper," *Energy*, vol. 189, p. 116199, 2019, doi: 10.1016/j.energy.2019.116199.

[4] S. Marcu, D. Popa, N. Stănescu, and N. Pandrea, "Model for the study of active suspensions," *IOP Conf. Ser. Mater. Sci. Eng.*, vol. 252, p. 012032, Oct. 2017, doi: 10.1088/1757-899X/252/1/012032.

[5] S. Gadadhe, A. More, and N. Bhone, "Experimental Analysis of Passive / Active Suspension System," *Int. Res. J. Eng. Technol.*, vol. 5, no. 11, pp. 703–707, 2018.

[6] M. R. Ahmed, A. R. Yusoff, and F. R. M. Romlay, "Adjustable Valve Semi-Active Suspension System for Passenger Car," *Int. J. Automot. Mech. Eng.*, vol. 16, no. 2, pp. 6470–6481, Jul. 2019, doi: 10.15282/ijame.16.2.2019.2.0489.

[7] M. Omar, M. M. El-kassaby, and W. Abdelghaffar, "A universal suspension test rig for electrohydraulic active and passive automotive suspension system," *Alexandria Eng. J.*, vol. 56, no. 4, pp. 359–370, Dec. 2017, doi: 10.1016/j.aej.2017.01.024.

[8] B. Ebrahimi, "Development of Hybrid Electromagnetic Dampers for Vehicle Suspension Systems," 2009.

[9] S. Kumar, A. Medhavi, and R. Kumar, "Active and Passive Suspension System Performance under Random Road Profile Excitations," *Int. J. Acoust. Vib.*, vol. 25, no. 4, pp. 532–541, Dec. 2020, doi: 10.20855/ijav.2020.25.41702.

[10] S. Li, J. Xu, X. Pu, T. Tao, H. Gao, and X. Mei, "Energy-harvesting variable/constant damping suspension system with motor based electromagnetic damper," *Energy*, vol. 189, no. April 2021, p. 116199, 2019, doi: 10.1016/j.energy.2019.116199.

[11] E. Diez-Jimenez, C. Alén-Cordero, R. Alcover-Sánchez, and E. Corral-Abad, "Modelling and Test of an Integrated Magnetic Spring-Eddy Current Damper for Space Applications," *Actuators*, vol. 10, no. 1, p. 8, Jan. 2021, doi: 10.3390/act10010008.

[12] T. M. Abdo, A. A. Huzayyin, A. A. Abdallah, and A. A. Adly, "Characteristics and analysis of an eddy current shock absorber damper using finite element analysis," *Actuators*, vol. 8, no. 4, 2019, doi: 10.3390/ACT8040077.

[13] H.J.J. Ho-Yeon Jung, In-Ho Kim, "Feasibility Study of the Electromagnetic Damper for Cable Structures Using Real-Time Hybrid Simulation," *sensors*, p. 2499, 2017, doi: 10.3390/s17112499.

[14] E. Diez-Jimenez, R. Rizzo, M.-J. Gómez-García, and E. Corral-Abad, "Review of Passive Electromagnetic Devices for Vibration Damping and Isolation," *Shock Vib.*, vol. 2019, pp. 1–16, Aug. 2019, doi: 10.1155/2019/1250707.

[15] Abdullah, J.-H. Ahn, and H.-Y. Kim, "Effect of Electromagnetic Damping on System Performance of Voice-Coil Actuator Applied to Balancing-Type Scale," *Actuators*, vol. 9, no. 1, p. 8, Feb. 2020, doi: 10.3390/act9010008.

[16] B. L. J. Gysen, J. J. H. Paulides, J. L. G. Janssen, and E. A. Lomonova, "Active Electromagnetic Suspension System for Improved Vehicle Dynamics," *IEEE Trans. Veh. Technol.*, vol. 59, no. 3, pp. 1156–1163, Mar. 2010, doi: 10.1109/TVT.2009.2038706.

[17] T. I. and K. A. A. J. Burhanudin, A.M. Ishak, A.S. Abu Hasim, "Permanent Magnet Linear Generator Design for Point Absorber Wave Energy Converter," 2019, doi: 10.1017/CBO9781107415324.004.

[18] P. Teli, V. Tamhankar, S. Zagade, and A. Suvre, "Study of Electromagnetic Damper," vol. 8, no. 09, pp. 708–711, 2019.

[19] Yong Yew Rong, "Simulation on Eddy Current Damper and its Regenerative," Universiti Tunku Abdul Rahman, 2013.

[20] H. a. Sodano, J.-S. Bae, D. J. Inman, and W. Keith Belvin, "Concept and model of eddy current damper for vibration suppression of a beam," *J. Sound Vib.*, vol. 288, no. 4–5, pp. 1177–1196, Dec. 2005, doi: 10.1016/j.jsv.2005.01.016.

[21] J. H. Kim, Y. J. Shin, Y. Do Chun, and J. H. Kim, "Design of 100W Regenerative Vehicle Suspension to Harvest Energy from Road Surfaces," *Int. J. Precis. Eng. Manuf.*, vol. 19, no. 7, pp. 1089–1096, Jul. 2018, doi: 10.1007/s12541-018-0129-5.

[22] B. Ebrahimi, M. B. Khamesee, and F. Golnaraghi, "A novel eddy current damper: theory and experiment," *J. Phys. D. Appl. Phys.*, vol. 42, no. 7, p. 075001, Apr. 2009, doi: 10.1088/0022-3727/42/7/075001.

[23] Siavash Haji Akbari Fini, "Theory and Simulation of Electromagnetic Dampers for Earthquake Engineering Applications," University of British Columbia, 2016.

[24] R. Rohith Renish, T. Niruban Projoth, K. Karthik, and K. Mohan Babu, "Vibration reduction in automobiles using electromagnetic suspension system," *Int. J. Mech. Eng. Technol.*, vol. 8, no. 8, pp. 729–737, 2017.

[25] S. Abu-Ein and S. M. Fayyad, "Electromagnetic Suspension System: Circuit and Simulation," *Int. J. Model. Optim.*, no. June 2019, pp. 440–444, 2013, doi: 10.7763/ijmo.2013.v3.316.

[26] L. A. J. Friedrich, B. L. J. Gysen, and E. A. Lomonova, “Modeling of Integrated Eddy Current Damping Rings for a Tubular Electromagnetic Suspension System,” in *2019 12th International Symposium on Linear Drives for Industry Applications (LDIA)*, Jul. 2019, pp. 1–4, doi: 10.1109/LDIA.2019.8770997.

[27] K. Hyniova, “On electromagnetic actuator control in the active suspension systems,” vol. 8, no. 1, pp. 6–8, 2020.

[28] P. V R, C. M. B N, and Y. S D, “Modified Electromagnetic Actuator for Active Suspension System,” *Int. J. Eng. Manag. Res.*, vol. 11, no. 4, pp. 188–193, 2021, doi: 10.31033/ijemr.11.4.23.

[29] D. Kong, D. Jiang, and Y. Zhao, “Electromagnetic suspension acceleration measurement model and experimental analysis,” *Electron.*, vol. 9, no. 2, pp. 1–13, 2020, doi: 10.3390/electronics9020226.

[30] S. Wayne, *Electricity, Magnetism and Light.* Academic Press, Amsterdam [etc.], 2008.

[31] E. Asadi, R. Ribeiro, M. B. Khamesee, and A. Khajepour, “A new adaptive hybrid electromagnetic damper: modelling, optimization, and experiment,” *Smart Mater. Struct.*, vol. 24, no. 7, p. 75003, 2015, doi: Artn 075003\r10.1088/0964-1726/24/7/075003.

[32] M. Montazeri and O. Kavianipour, “Investigation of the passive electromagnetic damper,” vol. 2646, no. September 2011, pp. 2633–2646, 2012, doi: 10.1007/s00707-012-0735-8.

[33] B. Ebrahimi, M. B. Khamesee, and F. Golnaraghi, “Permanent magnet configuration in design of an eddy current damper,” *Microsyst. Technol.*, vol. 16, no. 1–2, pp. 19–24, 2010, doi: 10.1007/s00542-008-0731-z.

[34] A. Fow and M. Duke, “Determining the volumetric characteristics of a passive linear electro-magnetic damper for vehicle applications,” *Cogent Eng.*, vol. 4, no. 1, p. 1374160, Jan. 2017, doi: 10.1080/23311916.2017.1374160.

[35] L. Zhu, C. R. Knospe, and S. Member, “Modeling of Nonlaminated Electromagnetic Suspension Systems,” *IEEE Trans. Mechatronics*, vol. 15, no. 1, pp. 59–69, 2010.

[36] Z. Li, L. Zuo, G. Luhrs, L. Lin, and Y. Qin, “Electromagnetic Energy-Harvesting Shock Absorbers : Design , Modeling , and Road Tests,” *IEEE Trans. Veh. Technol.*, vol. 62, no. 3, pp. 1065–1074, 2013, doi: 10.1109/TVT.2012.2229308.

[37] Q. Yang, Z. Chi, and L. Wang, “Influence and Suppression Method of the Eddy Current Effect on the Suspension System of the EMS Maglev Train,” *Machines*, vol. 10, no. 6, p. 476, 2022, doi: 10.3390/machines10060476.

[38] C. C. et al. J. L. Perez-Diaz, I. Valiente-Blanco, “A novel high temperature eddy current damper with enhanced performance by means of impedance matching,” *Smart Mater. Struct.*, vol. 28, no. 2, p. 025034, 2019.

[39] M. N. O. Sadiku, *Elements of Electromagnetics*, 7th editio. New York: Oxford University Press, 2018.

[40] B. Ebrahimi, M. B. Khamesee, and F. Golnaraghi, “Eddy current damper feasibility in automobile suspension: modeling, simulation and testing,” *Smart Mater. Struct.*, vol. 18, no. 1, p. 015017, 2009, doi: 10.1088/0964-1726/18/1/015017.

[41] J. Lau *et al.*, “Advanced systems and services for ground vibration testing - Application for a research test on an Airbus A340-600 aircraft,” *Proc. “IFASD 2011,”* no. January 2011, pp. 1–10, 2011.

[42] T. B. Mironova, A. B. Prokofiev, and V. Y. Sverbilov, “The Finite Element Technique for Modelling of Pipe System Vibroacoustical Characteristics,” *Procedia Eng.*, vol. 176, pp. 681–688, 2017, doi: 10.1016/j.proeng.2017.02.313.

[43] Anurag, “Diamagnetic Materials – Definition, Properties, Applications,” *geeksforgeeks.org*, 2021.